Title
Potential dual functional roles of the Y-linked RBMY in hepatocarcinogenesis

Journal
Cancer Science, 111(8)

ISSN
1347-9032

Authors
Kido, Tatsuo
Tabatabai, Z Laura
Chen, Xin
et al.

Publication Date
2020-08-01

DOI
10.1111/cas.14506

Peer reviewed

Received: 26 February 2020 | Revised: 20 May 2020 | Accepted: 22 May 2020

DOI: 10.1111/cas.14506

ORIGINAL ARTICLE

Cancer Science WILEY

Potential dual functional roles of the Y-linked RBMY in hepatocarcinogenesis

Tatsuo Kido[1,2] | Z. Laura Tabatabai[3] | Xin Chen[4,5] | Yun-Fai Chris Lau[1,2,5]

[1]Division of Cell and Developmental Genetics, Department of Medicine, San Francisco VA Health Care System, San Francisco, CA, USA

[2]Institute for Human Genetics, University of California, San Francisco, CA, USA

[3]Department of Pathology, San Francisco VA Health Care System, San Francisco, CA, USA

[4]Department of Bioengineering and Therapeutic Sciences, University of California, San Francisco, CA, USA

[5]Liver Center, University of California, San Francisco, San Francisco, CA, USA

Correspondence
Yun-Fai Chris Lau, Division of Cell and Developmental Genetics, Department of Medicine, San Francisco VA Health Care System and Institute for Human Genetics, University of California, San Francisco, CA 94121, USA.
Email: Chris.Lau@UCSF.edu

Funding information
U.S. Department of Defense, Grant/Award Number: CA150248; U.S. Department of Veterans Affairs, Grant/Award Number: 1 IK6BX004854 and 1 IO1BX004446

Abstract

Hepatocellular carcinoma (HCC) is a highly heterogeneous liver cancer with significant male biases in incidence, disease progression, and outcomes. Previous studies have suggested that genes on the Y chromosome could be expressed and exert various male-specific functions in the oncogenic processes. In particular, the RNA-binding motif on the Y chromosome (*RBMY*) gene is frequently activated in HCC and postulated to promote hepatic oncogenesis in patients and animal models. In the present study, immunohistochemical analyses of HCC specimens and data mining of The Cancer Genome Atlas (TCGA) database revealed that high-level *RBMY* expression is associated with poor prognosis and survival of the patients, suggesting that RBMY could possess oncogenic properties in HCC. To examine the immediate effect(s) of the RBMY overexpression in liver cancer cells, cell proliferation was analyzed on HuH-7 and HepG2 cells. The results unexpectedly showed that RBMY overexpression inhibited cell proliferation in both cell lines as its immediate effect, which led to vast cell death in HuH-7 cells. Transcriptome analysis showed that genes involved in various cell proliferative pathways, such as the RAS/RAF/MAP and PIP3/AKT signaling pathways, were downregulated by RBMY overexpression in HuH-7 cells. Furthermore, in vivo analyses in a mouse liver cancer model using hydrodynamic tail vein injection of constitutively active *AKT* and *RAS* oncogenes showed that RBMY abolished HCC development. These findings support the notion that Y-linked RBMY could serve dual tumor-suppressing and tumor-promoting functions, depending on the spatiotemporal and magnitude of its expression during oncogenic processes, thereby contributing to sexual dimorphisms in liver cancer.

KEYWORDS
hepatocellular carcinoma, RBMY, TCGA dataset, transcriptome analysis, Y chromosome

1 | INTRODUCTION

Liver cancer is one of the leading causes of cancer death worldwide. There are more than 840 000 new liver cancer cases and 780 000 cancer deaths from liver cancer each year, and the trends are increasing in recent years.[1-3] Hepatocellular carcinoma (HCC) is the most frequent primary liver cancer, accounting for 80%-90% of all cases.[4,5] Significantly, both the incidence and the

TABLE 1 Summary of the results of immunohistochemical analysis

Sample type	Sex	Samples	Number	RBMY immunohistochemistry		
				Densely positive	Sparsely positive	Negative
Tissue microarray	Male	NT	85	0	0	85 (100%)
		HCC	88	6 (6.8%)	11 (12.5%)	71 (80.7%)
	Female	NT	16	0	0	16 (100%)
		HCC	15	0	0	15 (100%)
Pathology preparation	Male	NT	43	0	0	43 (100%)
		HCC	43	7 (16.3%)	14 (32.6%)	22 (51.1%)
	Female	NT	6	0	0	6 (100%)
		HCC	6	0	0	6 (100%)

mortality of HCC are considerably higher in males than females with a ratio as high as 5.4 to 1, depending on the patient populations.[1,6,7] Both sex hormones and the sex chromosome genes have been postulated to contribute to such sex differences.[8-13] Various studies, including ours, have demonstrated that several Y chromosome genes, such as *testis-specific protein Y-encoded* (*TSPY*), *variable charge Y* (*VCY*), and *RNA-binding motif Y* (*RBMY*), are ectopically expressed in male HCCs at high frequency,[14-18] thereby potentially exerting male-specific functions in the oncogenic processes and contributing to sex differences in HCC patients. Indeed, overexpression of the putative Y-linked gonadoblastoma gene *TSPY* in HCC cells could promote cell proliferation and upregulate various cell-cycle regulators, including CDC25B, whose high expression levels are closely correlated with poor prognosis of HCC patients.[19]

Similar studies have suggested that high levels of RBMY expression could be associated with poor survival in HCC patients and promote oncogenesis in chemically induced mouse liver cancer models.[20,21] *RBMY* is a repetitive gene located within the azoospermia factor (*AZF*) region on the long arm of the human Y chromosome.[22] The coding sequences of respective copies, eg *RBMY1A1* and *RBMY1B*, are identical, hence here we term those copies as *RBMY* as a whole. RBMY is predominantly expressed in the male germ cells under normal conditions.[15,23] The encoded protein harbors an RNA-binding motif and could participate in RNA splicing events in germ cells of the testis.[24-27] Deletions in the *RBMY* genes cause failure in male meiosis, resulting in the absence of mature sperms in the testes of infertile patients.[23] RBMY is ectopically expressed in various somatic cancers, including lung adenocarcinoma, kidney renal papillary cell carcinoma, and hepatocellular carcinoma (HCC).[14] However, the roles of RBMY in cell proliferation, development, and oncogenesis are still unclear and somewhat controversial. For example, while RBMY is expressed in testicular germ cells, it is silent in testicular germ cell tumors (TGCT), such as seminoma and testicular embryonic carcinoma.[28] Furthermore, ectopic and epigenetic activation of RBMY inhibited proliferation of embryonic stem cells, resulting in embryonic lethality in mouse.[29] Conversely, RBMY is abundantly expressed in selected HCC specimens and its cytoplasmic location in tumor cells is associated with poor clinical outcomes in patients.[20] These observations suggested that RBMY could serve dual functions in oncogenesis, ie tumor-promoting and tumor-suppressing functions, depending on its expression levels and spatiotemporal patterns in the processes.

In the present study, we investigated the expression patterns of RBMY in clinical HCC specimens by immunohistochemistry and explored the immediate effects of RBMY overexpression in a hepatocellular carcinoma cell line HuH-7 and a hepatoblastoma cell line HepG2 using the tet-ON conditional gene activation system,[30] and transcriptome[19,31] and pathway analyses.[32,33] In vivo effects of RBMY overexpression were further studied using the constitutively active *AKT* and *RAS* oncogene-induced mouse liver cancer model and the hydrodynamic transfection technique.[34-36] Our results showed that RBMY is differentially expressed in heterogeneous patterns with densely and sparsely positive as well as negative immunostaining patterns in pathological male specimens. High-level RBMY expression is associated with poor survival of HCC patients. However, RBMY overexpression showed immediate inhibitory effects on cell proliferation in both HuH-7 and HepG2 cells. Transcriptome and pathway analyses revealed that overexpression of RBMY could downregulate various genes involved in cell proliferation, particularly affecting the RAS/RAF/MAP and PIP3/AKT signaling pathways. Significantly, RBMY completely abolished tumor formation in the *AKT* and *RAS* oncogene-induced liver cancer model, compared with positive controls without RBMY. Our findings suggested the possibility that RBMY could possess dual oncogenic/anti-oncogenic functions in promoting and suppressing hepatocarcinogenesis respectively in spatiotemporal and dosage-dependent manners.

2 | MATERIALS AND METHODS

2.1 | Human hepatocellular carcinoma specimens

Tissue microarrays of human HCC and normal liver tissues were purchased from US BioMax (Derwood, MD),

comprising information from 101 patients with HCC (85 males and 16 females) and 103 patients with adjacent normal liver tissue (85 males and 16 females) (Table 1). Human pathology HCC specimens were obtained from the VA Medical Center-University of California, San Francisco, and the Cooperative Human Tissue Network, consisting of 43 male cases and 6 female cases (Table 1). The studies were performed under an exempted protocol, approved by the Institutional Committee on Human Research.

2.2 | Lentiviruses and cell culture

cDNA coding for human RBMY was cloned into the *Eco*RI site of the lentiviral plasmid *FUW-tetO*[37] (Addgene), resulting in the *FUW-tetO-RBMY* construct. An enhanced green fluorescent protein (EGFP) expression vector *FUW-tetO-EGFP*, that harbored an IRES-EGFP cassette was used as a control. Lentiviruses for the expression of RBMY and EGFP with the tet-ON system were prepared as described previously.[19,38] Human HCC HuH-7 and hepatoblastoma HepG2 cells were transduced with lentiviruses.[19,38] Transgene expression was induced by addition of 0.5 μg/mL doxycycline (Dox) in the culture medium. Cell proliferation assay and annexin-V binding assay were performed as before.[19,31]

2.3 | Mouse liver cancer model using hydrodynamic tail vein injection

The plasmid vectors for the mouse HCC model using the hydrodynamic injection technique have been described previously; ie *pT3-EF1α-HA-myr-Akt* (designated as *pT3-AKT*^{myr}), *pT2CAGGS-NRasV12* (designated as *pT2-NRAS*^{V12}), *pCMV/sleeping beauty transposase* (designated as *pCMV-SB*), and *pT3-EF1α* (empty vector).[35,36] The coding sequence of human RBMY was inserted into the *pT3-EF1α* plasmid using the Gateway LR clonase II system, resulting in *pT3-EF1α-RBMY* (designated as *pT3-hRBMY*). EGFP expression plasmid vector *pT3-EF1α-EGFP* (designated as *pT3-EGFP*) was used as a control.

FVB male mice were divided randomly into 3 groups of 5-7 animals each. Hydrodynamic injection was performed as described previously.[35,36] In brief, 10 μg *pT3-AKT*^{myr}, 10 μg *pT2-NRAS*^{V12}, 2 μg *pCMV-SB*, and 30 μg *pT3-RBMY* or *pT3-EGFP* were diluted in 2 mL saline (0.9% NaCl), sterilized through 0.2-μm filter and injected into the lateral tail vein of a recipient mouse (20 g body size) in 7 s. The injected transgenes could co-integrate into the genome of selected hepatocytes and stably express in the liver of the recipients. Animals were monitored twice weekly for tumor growth, harvested at 8 wk post-injection, and analyzed by necropsy, pathological evaluation, histochemistry, and immunohistochemistry. The Institutional Animal Care and Use Committee approved all experimental procedures accordingly to the NIH Guide for Care and Use of Laboratory Animals.

2.4 | Western blotting, immunohistochemistry, and immunofluorescence

Western blot analysis was performed as described previously.[39] Immunohistochemistry and immunofluorescence were performed using an anti-RBMY rabbit monoclonal IgG (clone R12508(2), Abcam), anti-Ki-67 rabbit monoclonal IgG (clone SP6, ThermoFisher Scientific), anti-glypican 3 (GPC3) mouse monoclonal IgG (clone 4A5, BioMosaics, Burlington, VT), anti-LIN28B rabbit monoclonal IgG (clone EPR18717, Abcam), anti-GFP (Abcam) or anti-TSPY mouse monoclonal IgG (in-house), as described previously.[40,41]

2.5 | RNA preparation and RNA-Seq transcriptome analyses of the transduced HuH-7 cells

RNA-Seq transcriptome analyses of HuH-7 cells, expressing RBMY or EGFP alone after 24-h induction, were performed in biological triplicates using 1 μg total RNA per sample. Sequencing libraries were bar coded and sequenced on the Illumina NextSeq 500 sequencer.[19,31]

Approximately 20 million sequence reads per sample were mapped onto the Ensembl GRCh37/UCSC hg19 human reference genome using TopHat software.[19,31] Expression levels were calculated using the featureCounts program.[42] Differential gene expression analysis was performed using an R package for Tag Count Comparison (TCC) program.[43]

Differentially expressed genes between HuH-7 cells expressing RBMY and EGFP were divided into upregulated and downregulated groups. Gene ontology and pathway analyses were performed using the DAVID Bioinformatics Resources 6.8 (https://david.ncifcrf.gov/), and the Kyoto Encyclopedia of Genes and Genomes (KEGG) and REACTOME databases.[32,33,44,45]

2.6 | Dataset and data mining analysis of HCC specimens from TCGA

Normalized and processed RNA-Seq gene expression data and corresponding clinical information for the HCC patients at The Cancer Genome Atlas (TCGA) data portal were downloaded from the UCSC Xena Browser.[46] The dataset included information from 22 patients with male nontumor samples, 250 patients with male HCCs, 28 patients with female nontumor samples, and 121 patients with female HCCs. Male HCC cases were classified based on their RBMY expression levels: RBMY-high group (threshold = 100 RSEM normalized count, n = 26), RBMY-low group (0 < expression level < 100 RSEM normalized count, n = 51), and RBMY-negative group (expression level = 0 RSEM normalized count, n = 173).

Statistical analyses were performed using the Prism8 program (GraphPad Software). Survival analysis for the HCC cases in TCGA datasets was performed using data from the Human Protein Atlas

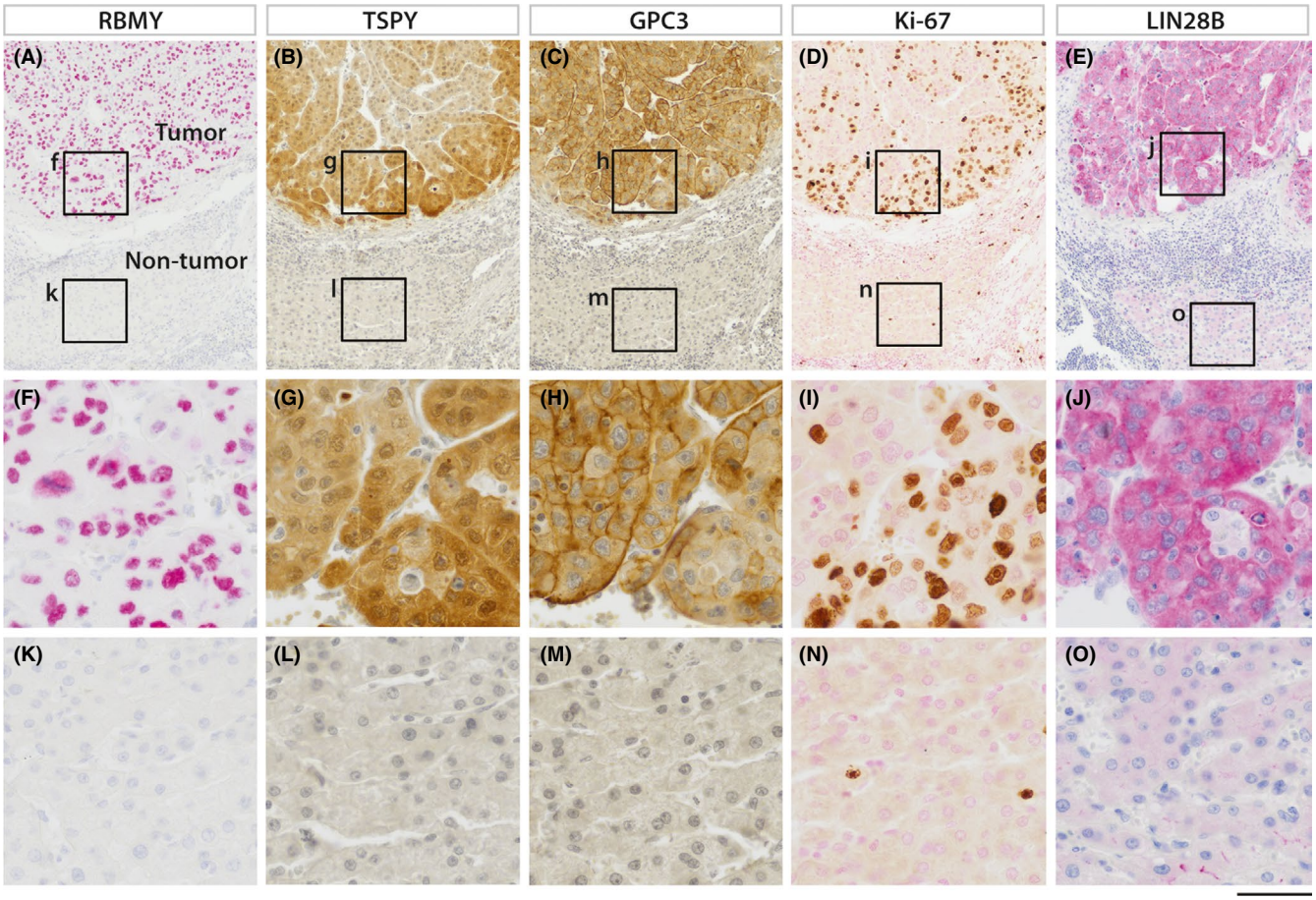

FIGURE 1 Expression of RNA-binding motif, Y (RBMY), testis-specific protein, Y (TSPY), and the tumor markers glypican 3 (GPC3), Ki-67, and LIN28B in a representative male hepatocellular carcinoma specimen. The boxed areas in A-E representing tumor (f-j) and non-tumor (k-o) areas are magnified in (F-J) and (K-O) respectively. Nuclei were counterstained by hematoxylin (A-C, E) and Nuclear Fast Red (D). See text for details. Bar represents 200 μm in (A-E), 50 μm in (F-O)

(HPA).[47] Expression levels of RBMY and Ki-67 were correlated with the respective patient survival in days.

3 | RESULTS

3.1 | RBMY expression in hepatocellular carcinoma specimens

Previous studies, including ours, have shown that RBMY is aberrantly expressed together with other Y chromosome genes, such as *TSPY* and *VCY*, and other oncogenes, such as *LIN28B*, and cell proliferative markers, *Ki-67*, in HCC specimens.[14,40] Initially, we studied the RBMY expression pattern using immunohistochemistry with reference to other tumor markers, such as GPC3 and LIN28B, the Y-located gonadoblastoma gene *TSPY* and the proliferative marker Ki-67, in selected HCC specimens. The results showed that RBMY is expressed primarily in the nuclei of tumor cells and is frequently co-expressed with these markers in tumors and not in the adjacent nontumor (NT) areas (Figure 1). No cytoplasmic RBMY expression was observed in our HCC samples. TSPY was expressed in both the cytoplasm and nuclei; GPC3 was located in the cytoplasm and cellular membrane; Ki-67 was nuclear located, and LIN28B was located in the cytoplasm, as previously reported.[40,48-51] Next, we analyzed the RBMY expression patterns in more detail using both tissue microarrays (TMAs) and pathological HCC specimens (Table 1). Analysis of

FIGURE 2 Differential expression of RNA-binding motif, Y (RBMY) in male hepatocellular carcinoma (HCC) specimens. A, Three types of the RBMY expression patterns: (i) densely positive (left column), (ii) sparsely positive (middle 2 columns), and (iii) negative (right column). Middle row shows magnified images of the boxed areas and bottom row shows negative staining of adjacent nontumor areas. B, Top row, example of RBMY-densely positive (B1) and Ki-67 (B2) staining of adjacent sections. B3 and B4 show the magnified images of the boxed area in (B1) and (B2) respectively. C, Example of RBMY-sparsely positive (C1) and Ki-67 (C2) staining in the adjacent sections. Bottom panels (C3-C6) show magnified images of the boxed areas (c3-c6) on the top panels respectively. Only RBMY-densely positive tumor cells could be correlated with Ki-67 expression. Bars represent 100 μm

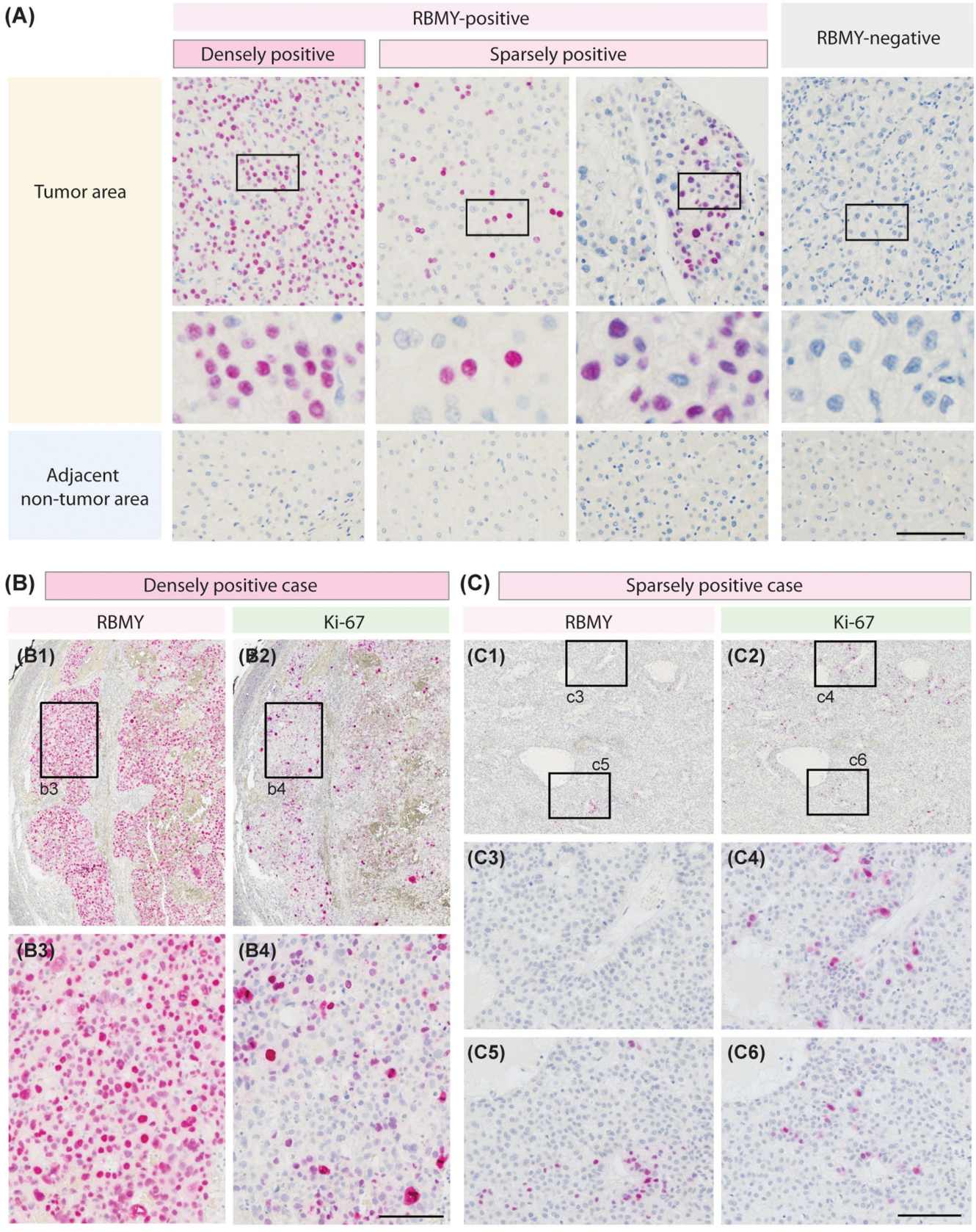

HCC specimens from 131 male and 21 female patients and adjacent NT specimens revealed 3 types of immunohistochemical patterns for RBMY: (i) densely positive (RBMY densely), (ii) sparsely positive (RBMY sparsely), and (iii) negative (RBMY negative) (Figure 2A), while all NT areas and HCC samples from female patients were negative for RBMY expression. In the tissue microarray samples, RBMY

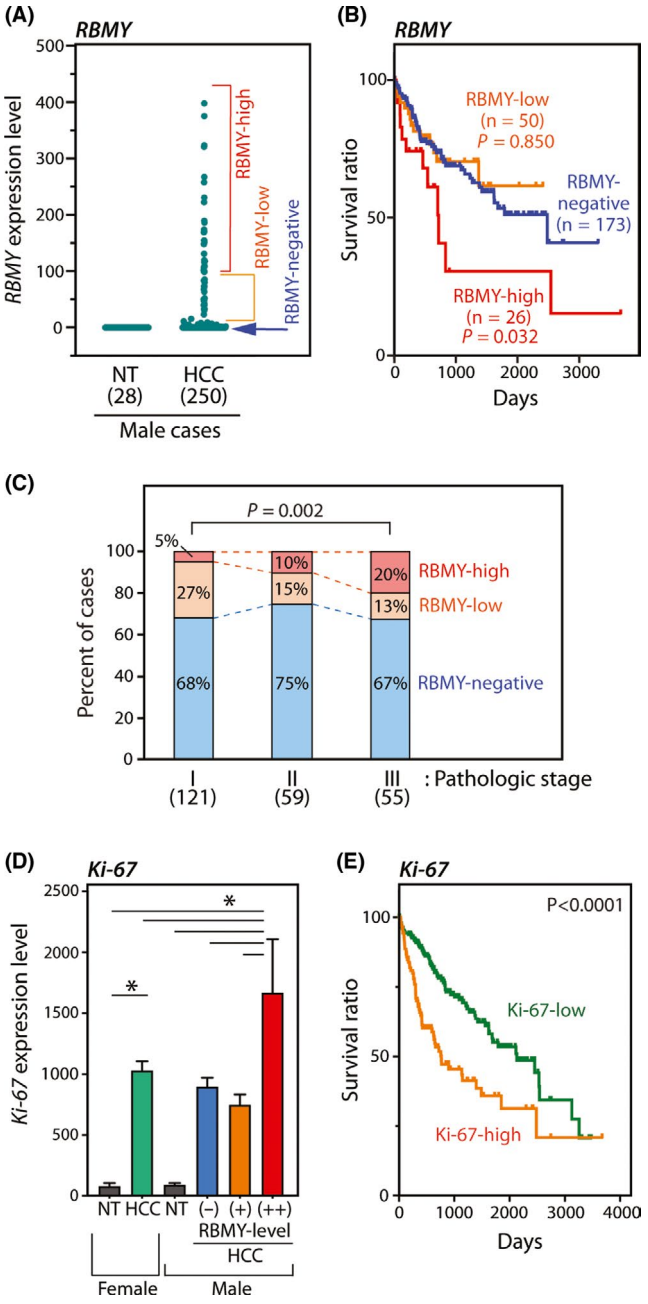

FIGURE 3 Expression analysis of RNA-binding motif, Y (RBMY) and Ki-67 in the transcriptomes of hepatocellular carcinoma (HCC) specimens in The Cancer Genome Atlas (TCGA) database. A, Plot of RBMY relative expression levels in male HCC transcriptomes, showing the RBMY-high, RBMY-low, and RBMY-negative groups. NT, nontumor tissues; the number in parentheses indicates the respective sample size. B, Kaplan-Meier survival plot showing the survival rates of the male RBMY-high (red), male RBMY-low (orange), and male RBMY-negative (blue) groups. Log-rank test *P*-values against RBMY-negative group are indicated. RBMY-high expression is associated with poor survival of the patients. C, Ratios of RBMY-high, RBMY-low, and RBMY-negative groups at respective HCC pathological stages. Chi-square test *P*-value is indicated. There is a gradual increase (ie from 5% to 20%) in the proportion of RBMY-high expression level toward later pathologic stages. D, The expression levels of Ki-67 in the nontumor (NT) and HCC samples of female (left) and male (right) HCC groups negative (–), low (+) and high (++) for RBMY expression respectively. Asterisks indicate *t* test *P*-value < .05. Ki-67 expression is further elevated in RBMY-high expression HCC group. E, Kaplan-Meier survival plot showing the survival rate of the Ki-67-high group (orange) and Ki-67-low group (green). Log-rank test *P*-value is indicated. High Ki-67 expression is associated with poor survival of the patients

was expressed at 6.8% in densely positive, 12.5% in sparsely positive and 80.7% negative sections respectively. Among the larger pathology preparations of HCC specimens, RBMY was expressed at 16.3% in densely positive, 32.6% in sparsely positive and 51.1% negative sections respectively (Table 1). We surmised that the relatively large sizes of the pathology preparations could have accounted for the higher positive staining compared with those of small TMA HCC samples. Most densely positive HCC specimens overlapped significantly (Figure 2B) while the sparsely positive and RBMY-negative HCC cases did not overlap with the Ki-67 staining patterns (Figure 2C), suggesting a likely correlation of densely and sparsely positive RBMY expression with relatively high and low cell proliferative properties among the HCC specimens from male patients.

3.2 | High level of RBMY expression is associated with poor prognosis of the HCC patients

To explore the potential association of the differential *RBMY* expression levels to those of clinical outcomes, we performed a data mining study with transcriptome datasets of specimens from 250 male and 121 female patients with HCC, as well nontumor specimens from 22 male and 28 female patients with patient survival information from TCGA database.[52] The expression levels of *RBMY* in the HCC transcriptomes/specimens were classified as high, low and negative (Figure 3A), and correlated to patient survival in days. The results showed that the survival ratio of male patients with HCC expressing *RBMY* at a high level was significantly lower than those of men in the RBMY-low and RBMY-negative groups (Figure 3B). There was little difference between the RBMY-low and RBMY-negative groups. Although the proportion of RBMY-negative patients did not change significantly with various pathologic stages (I-III), ie within 67% to 75% range, there seemed to be an increase in the proportion of RBMY-high expression patterns toward the later stages, ie from 5% to 20% (Figure 3C). Furthermore, the expression of the cell proliferative marker *Ki-67* was relatively higher in HCC tumor specimens (Figure 3D) and is usually correlated with poor patient survival (Figure 3E). Interestingly, *Ki-67* expression levels did not show any significant differences among specimens from the female, RBMY-negative (–) and RBMY-low (+) male patients with HCC, while there was a statistically significant increase in *Ki-67* expression in samples from RBMY-high (++) male patients with HCC (Figure 3D), suggesting that high *RBMY* expression is correlated with increased cell proliferation and poor survival of the patients (Figure 3B,D,E).

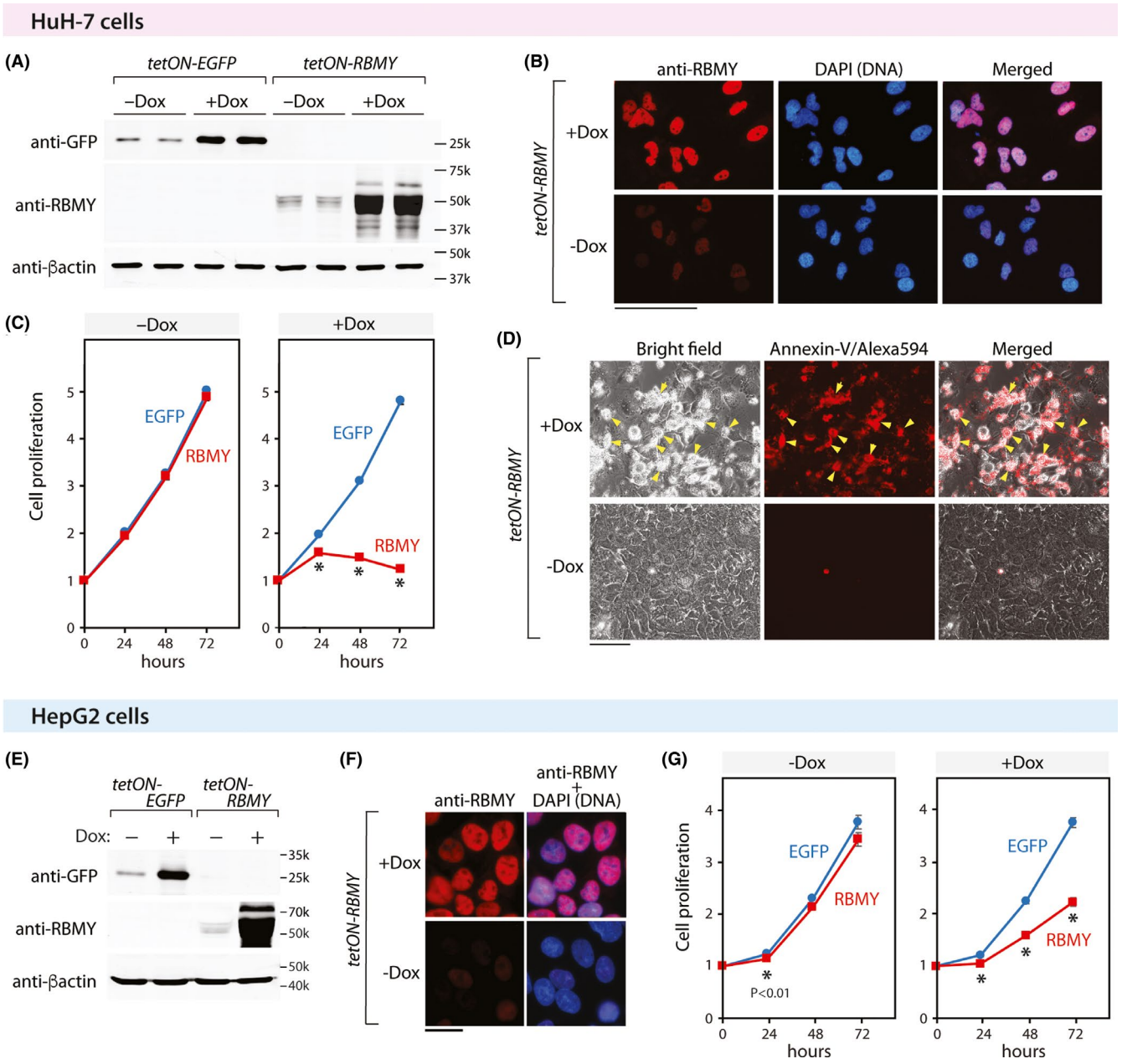

FIGURE 4 RNA-binding motif, Y (RBMY) overexpression inhibits cell proliferation in HuH-7 (top panels) and HepG2 (bottom panels) cells. A, E, Western blots of EGFP and RBMY in the transduced HuH-7 (A) and HepG2 cells (E) at 1 d post–Dox induction (+Dox). β-Actin was used as an internal control. −Dox indicates noninduced cells. B, F, Immunofluorescence showed that the activated RBMY (red, +Dox) was localized in the nuclei of RBMY-transduced (tet-ON-RBMY) HuH-7 (B) and HepG2 (F) (+Dox). DNA was visualized by DAPI staining (blue). C, G, Cell proliferation assays showed that overexpression of RBMY in HuH-7 and HepG2 cells significantly inhibited cell proliferation, as compared with EGFP alone (+Dox, right). There was no difference between transduced RBMY and enhanced GFP (EGFP) cells under noninduced conditions (−Dox, left). Asterisks indicate *t* test *P*-value < .05. D, Annexin-V binding assay at 72 h post–Dox induction showing detached tet-ON-RBMY HuH-7 cells being annexin-V positive (red), corresponding to dead cells. Bars represent 100 μm in (B, D), and 20 μm in (F)

3.3 | Conditional RBMY overexpression retards cell proliferation in HuH-7 and HepG2 cells

To explore the immediate effects of overexpression of human RBMY in HCC, we used a lentiviral vector-mediated tet-ON system to conditionally overexpress RBMY in the HCC cell line, HuH-7, and hepatoblastoma cell line, HepG2. Under this system, the transgene could be activated in the transduced cells with the addition of Dox in the culture medium.[30] The green fluorescent protein (*EGFP*) transgene was used as a control. Western blotting was used to confirm the expression of the respective transgenes in the induced cells (Figure 4A,E). Immunofluorescence analyses showed that the overexpressed RBMY protein was predominantly localized in the nuclei of transduced cells (Figure 4B,F), consistent with the observation in clinical HCC samples (Figures 1 and 2). Cell proliferation assays showed that, under induction conditions (+Dox), cell proliferation of the HuH-7 and HepG2 cells

TABLE 2 Pathways enriched with the genes downregulated by RBMY overexpression in HuH-7 cells. Pathways were identified by DAVID with KEGG and REACTOME databases

Pathway	Database	Molecule	*P-value*	Genes in cluster
Cluster 1, Enrichment score = 2.27				
Hippo signaling pathway	KEGG	14	7.89E-05	*BIRC3*, *BMP2*, *BMP4*, *BMP8B*, *BMPR2*, *CDKN2B*, *CER1*, *COL4A5*, *CTGF*, *CXCL8*, *CXCR4*, *DKK1*, *EDN1*, *EGF*, *ERBB4*, *FGF12*, *FRAT1*, *FZD1*, *FZD5*, *FZD6*, *FZD8*, *FZD9*, *HIF1A*, *IGF1R*, *INHBB*, *ITGA2*, *LPAR6*, *LUM*, *PDGFB*, *PLCE1*, *PPP1R12B*, *PTGER4*, *PTH2R*, *TEAD2*, *TGFB2*, *TGFB3*, *WNT3*
Pathways in cancer	KEGG	23	2.26E-04	
Basal cell carcinoma	KEGG	8	3.19E-04	
R-HSA-373080: Class B/2 (Secretin family receptors)	REACTOME	7	6.87E-04	
Proteoglycans in cancer	KEGG	14	1.23E-03	
Signaling pathways regulating pluripotency of stem cells	KEGG	11	2.25E-03	
R-HSA-5340588: RNF mutants show enhanced WNT signaling and proliferation	REACTOME	3	1.30E-02	
Wnt signaling pathway	KEGG	9	2.00E-02	
Melanogenesis	KEGG	7	3.60E-02	
Cluster 2, Enrichment score = 1.84				
R-HSA-380108: Chemokine receptors bind chemokines	REACTOME	9	4.88E-05	*BMP2*, *BMPR2*, *CCL20*, *CCR1*, *CCRL2*, *CXCL1*, *CXCL3*, *CXCL5*, *CXCL6*, *CXCL8*, *CXCR4*, *IL18*, *INHBB*, *OSMR*, *TGFB2*, *TGFB3*, *TNFRSF21*
Cytokine-cytokine receptor interaction	KEGG	16	8.86E-04	
Rheumatoid arthritis	KEGG	7	2.08E-02	
Cluster 3, Enrichment score = 1.32				
R-HSA-2219530: Constitutive signaling by aberrant PI3K in cancer	REACTOME	7	2.44E-03	*BTC*, *EGF*, *ERBB4*, *IRS2*, *KL (klotho)*, *KLB*, *PDGFB*
R-HSA-1257604: PIP3 activates AKT signaling	REACTOME	7	9.84E-03	
R-HSA-1236394: Signaling by ERBB4	REACTOME	3	2.44E-02	
R-HSA-5673001: RAF/MAP kinase cascade	REACTOME	7	4.74E-02	
Cluster 4, Enrichment score = 1.29				
R-HSA-3000178: ECM proteoglycans	REACTOME	7	6.82E-03	*BMP2*, *BMP4*, *COL4A5*, *ITGA2*, *ITGB6*, *LUM*, *MATN3*, *TGFB2*, *TGFB3*
R-HSA-2129379: Molecules associated with elastic fibers	REACTOME	5	1.02E-02	

overexpressing RBMY was drastically retarded, as compared with those of the corresponding EGFP control cells and those cells without induction (−Dox) (Figure 4C, G). At 3-d post–Dox induction, numerous HuH-7 cells overexpressing RBMY were strongly stained by annexin-V, suggesting a significant apoptosis/cell death among these cells (Figure 4D, red fluorescence). Interestingly, extended activation of the *RBMY* transgene resulted in the emergence of HuH-7/HepG2 cells with restored normal proliferative properties compared with that of the control cells (data not shown). These results suggested that overexpression of RBMY impaired cell proliferation in the short term, while persistent RBMY expression promoted evolutionary adaptation and restoration of proliferative properties of the tumor cells.

3.4 | RBMY downregulated various genes in the cancer-associated pathways in HuH-7 cells

As overexpression of RBMY induced immediate inhibitory effects on cell proliferation and promoted cell death in HuH-7 cells (Figure 4C,D), using a RNA-Seq strategy we sought to determine its effects on gene expression in the RBMY-overexpressing HuH-7 cells as compared with those of EGFP control cells. Total RNA was extracted from the respective cell populations after 24-h doxycycline induction and in biological triplicates subjected to RNA-Seq analysis, as described previously.[19,31] Our results identified 1093 differentially expressed genes (DEGs) between RBMY and EGFP overexpressed cells, consisting of 523 upregulated genes and 570 downregulated genes, with FDR < .01 by TCC analysis, expressing levels of $\log_2$[read count]>1, and |$\log_2$[fold change]|> 0.8 (Table S1).[43] Pathway analyses using the DAVID Bioinformatics Resources [32,33,44,45] showed that various signaling pathways, including RAS/RAF/MAP and PIP3/AKT signaling pathways, and other pathways, such as Hippo and WNT signaling pathways, associated with various aspects of oncogenesis,[53-57] were enriched among the genes downregulated by RBMY overexpression (Table 2). RBMY downregulated several factors involved in the activation of the RAS/RAF/MAP and PIP3/AKT signaling pathways, including *BTC*, *EGF*, *ERBB4*, *PDGFB*, and *KLB*. In contrast, similar pathway analysis resulted in no statistically

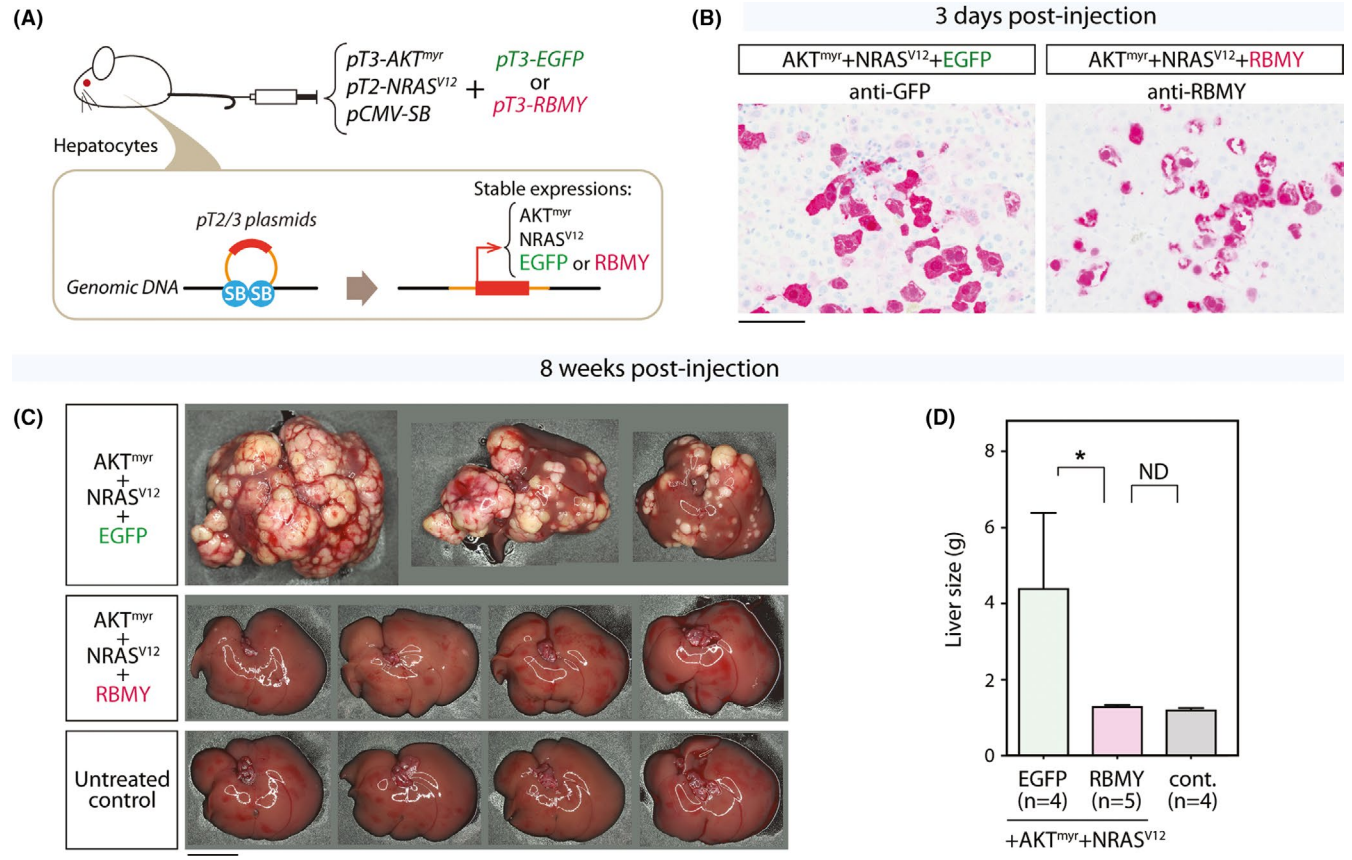

FIGURE 5 RNA-binding motif, Y (RBMY) overexpression abolishes tumor formation in a mouse liver cancer model mediated by constitutively active *AKT*^{myr} and *NRAS*^{V12} oncogenes. A, Schematic diagram illustrating the hydrodynamic transfection of the oncogenes in the mouse liver using the Sleeping Beauty (SB) transposon system. DNAs inserted in either *pT2* or *pT3* vectors are capable of integrating into the hepatocyte genome mediated by SB transposase encoded by the *pCMV-SB* plasmid, when they are hydrodynamically co-injected via the tail vein of the recipient mouse. Using the constitutively active *AKT*^{myr} and *NRAS*^{V12} oncogenes, such integration results in transformed hepatocytes that become tumorigenic and develop into loci of hepatocellular carcinoma (HCC) in 8 wk post-injection. The effects of RBMY in such oncogenic processes are evaluated in this system by inclusion of either *pT3-RBMY* or *pT3-EGFP* (control) plasmid in the injection mixtures. B, Immunohistochemistry showing the expression (red) of enhanced GFP (EGFP) (anti-GFP) and RBMY (anti-RBMY) in the respective transfected livers of the recipients at 3 d post-injection. C, Gross morphological images of selected livers from AKT^{myr}/NRAS^{V12}/EGFP, AKT^{myr}/NRAS^{V12}/RBMY, and untreated control mice at 8 wk post-injection. The constitutively active *AKT*^{myr} and *NRAS*^{V12} oncogenes induced foci of tumors with EGFP control plasmid (top row) while inclusion of a RBMY expression vector abolished such tumor formation (middle row) similar to untreated controls (bottom row). Bar represents 1 cm. D, Average liver weight of the mice corresponding to the results of an experiment, as presented in (C). Asterisk indicates Mann-Whitney test *P*-value < .05, and numbers in parentheses indicate the respective sample size. Bar indicates the standard error of each group. ND, no difference

significant pathways being identified among the upregulated genes (data not shown). Hence, transcriptome and pathway analyses supported the observations of of cell proliferation and oncogenic signaling by RBMY overexpression in HuH-7 cells (Figure 4C,D).

3.5 | RBMY overexpression inhibits oncogene-induced HCC development in an in vivo mouse model

The AKT and RAS signaling pathways are frequently activated and associated with cancer development in human HCC.[58-61] Aberrant activation of these pathways is widely involved in initiation and progression of various cancer types.[59,62-64] Indeed, co-activation of the AKT and RAS pathways in mouse liver cancer models promotes rapid carcinogenesis.[34,65] In the present study, we investigated the in vivo effects of RBMY in the *AKT* and *RAS* oncogene-induced liver cancer model using a hydrodynamic tail vein injection technique. Hydrodynamic tail vein injections of DNA in mice result in delivery of the injected DNA primarily to the liver of the recipient hosts.[34-36] When such DNAs are flanked by the Sleeping Beauty (SB) inverted/direct repeat sequences (IR/DR) and co-injected with the SB transposase expression cassette, they could be efficiently integrated into the genome of hepatocytes (Figure 5A).[35,36] By hydrodynamic injection of the expression vectors harboring the constitutively active *AKT* (*pT3-AKT*^{myr}) and *NRAS* (*pT2-NRAS*^{V12}) oncogenes with SB vector (*pCMV-SB*), selected hepatocytes could be transformed into tumor cells within 8 wk post-injection, thereby forming foci of HCC in host animals.[35,36] To evaluate the effects

of the human RBMY in this in vivo HCC mouse model, we produced groups of co-injected mice with a combination of *pT3-AKT^{myr}*, *pT2-NRAS^{V12}*, *and pCMV-SB*, and either with (a) a RBMY expression vector *pT3-RBMY* (AKT^{myr}/NRAS^{V12}/RBMY mice), or (b) an EGFP expression vector *pT3-EGFP* (AKT^{myr}/NRAS^{V12}/EGFP mice) (Figure 5A). The latter served as a positive control, while non-injected animals served as negative controls. Initially, immunohistochemistry was performed on the livers of recipient mice at 3 d post-injection, which confirmed the efficient uptake of the co-injected DNAs and hepatic expression of the transgene *EGFP* and *RBMY* respectively (Figure 5B). At 8 wk post-injection, the positive control group of mice (AKT^{myr}/NRAS^{V12}/EGFP) developed significant HCCs, while none of the AKT^{myr}/NRAS^{V12}/RBMY mice developed any HCC in their livers, similar to the findings in the untreated negative control (Figure 5C, top, middle, and bottom row respectively). These observations were obtained consistently in 3 separate experiments with groups of 4-6 animals each. Figure 5D represents measurements of the weights of the livers of experimental animals from one of these studies, showing an increase in the average weight of the positive control mice (AKT^{myr}/NRAS^{V12}/EGFP) while those for AKT^{myr}/NRAS^{V12}/RBMY mice were similar to that of untreated negative controls. These results suggested that early expression of RBMY could inhibit/suppress the initiation of tumorigenesis mediated by constitutively active *AKT^{myr}* and *NRAS^{V12}* oncogenes in this in vivo animal model of HCC.

4 | DISCUSSION

The human sex chromosomes, ie X and Y, evolved from a pair of identical chromosomes, through which one of them acquired a sex-determining gene and became the Y chromosome while the other one became the X chromosome.[66] In particular, the male-specific region on the Y chromosome (MSY) harbors genes that serve specific functions pertaining to male sex determination, differentiation, and/or physiology.[67] In total, 24 X degenerate/transposed or ampliconic genes are located on MSY, most of which have an X homolog with highly conserved sequences and encoded proteins that are capable of serving similar functions.[67-69] There are a few exceptions, ie the sex-determining gene *SRY*, the gonadoblastoma gene *TSPY* and *RBMY*, whose X homologs, ie *SOX3*, *TSPX*, and *RBMX* respectively, encode for somewhat diverged proteins and might possess different functions from their respective Y counterparts.[15,23,70-72] Most conserved MSY and their X homologs are expressed ubiquitously in a wide variety of tissues, while those of diverged MSY genes are primarily expressed in the testis, ie *SRY*, and/or germ cells, ie *TSPY* and *RBMY*, and are likely to play crucial roles in male sex determination/differentiation and spermatogenesis.[15,23,70,73] Ectopic expression of MSY genes in other somatic tissues/organs could contribute sex differences in normal development, differentiation and physiology,[67] and disease initiation, progression, and treatment responses in male-biased manners.[15,71] Indeed, ectopic expression of testis-specific genes, ie *SRY*, *TSPY*, and *RBMY*, have been observed in normal and diseased somatic cells/tissues, and have been postulated to exert male-specific actions on the normal and/or diseased development.[14-16,38,74,75]

Hepatocellular carcinoma is a major liver cancer, which shows significant male predominance in incidence and mortality.[1,4-7] Although such sex differences have been attributed to the differential actions of sex hormones and their receptors, in which the male sex hormone androgen/receptors and the female sex hormone estrogen/receptors are postulated to exacerbate and suppress the various aspects of hepatocarcinogenesis,[12,76-79] genetic factors, particularly those encoded by the MSY genes, could also contribute to the pathogenic processes.[15,67,71,80] Various studies have demonstrated that *TSPY*, *VCY*, and *RBMY*, are ectopically and highly expressed in selected HCC, thereby contributing to differential gene regulatory program(s) and sex differences in HCC.[14,16-18,20,21,40,81]

RBMY protein harbors an RNA recognition motif (RRM) and functions as a regulator of germ cell-specific splicing events.[24-27] Although it shares a conserved RRM domain with its X homolog RBMX, they diverged at their flanking sequences. RBMX is ubiquitously expressed, including in the liver, and plays fundamental roles in the DNA-damage response and regulation of chromatid cohesion as well as in RNA splicing activity.[82-86] Hence, RBMY and RBMX could serve slightly different biological functions. Accordingly, ectopic expression of RBMY could exert male-specific functions on hepatocarcinogenesis. Our immunohistochemistry analysis on clinical HCC specimens revealed 3 RBMY expression patterns, in which the RBMY-densely expression pattern is associated with the proliferative marker Ki-67, but not those sparsely positive/negative expression patterns. We surmised that densely positive and sparsely positive/negative specimens could correspond to those RBMY-high and those RBMY-low/negative samples in the TCGA transcriptomes, the former of which is associated with poorer patient survivals than the latter. Interestingly, we detected a RBMY protein location primarily on the nuclei of tumor cells, while others suggested that only cytoplasmic location of the RBMY protein is associated with poor prognosis of the patients.[20,21] At present, we are uncertain of the reason(s) for such difference(s) in the cytological locations of the RBMY proteins in the tumor cells. Nevertheless, high RBMY expression is associated with poor outcomes for the patients.

Our in vitro and in vivo assays demonstrated that overexpression of RBMY suppresses cell proliferation in cultured liver cancer cells and completely abolishes hepatocarcinogenesis in an acute oncogene-induced mouse HCC model (Figures 4 and 5). These observations seem to be in contrast with those of clinical data, suggesting that RBMY-high expression is associated with cell proliferative marker, Ki-67, and poor prognosis of the patients. We surmised that the suppression of cell proliferation and promotion of cell death are immediate effects upon induction of the *RBMY* transgene in the culture cells. Our transcriptome and pathway analyses suggested that such RBMY overexpression inhibits various oncogenic pathways, including Wnt, Hippo, PIP3/AKT and RAS/RAF/MAP signaling pathways, in HuH-7 cells (Table 2). Using an acute in vivo HCC model mediated

by constitutively active AKT^{myr} and $NRAS^{V12}$ oncogenes, we further demonstrated that overexpression of RBMY inhibited the initiation of oncogenesis in the transfected hepatocytes in the livers of recipient mice. Importantly, both AKT and RAS signaling pathways are inhibited similarly as immediate effects of RBMY overexpression in HuH-7 cells. The AKT^{myr} and $NRAS^{V12}$ oncogenes transformed selected hepatocytes upon initial transfection to the liver by hydrodynamic tail vein injection, and such transformed tumor cells developed into foci of HCC in 8 wk. The co-injected RBMY could have an immediate effect(s) in abolishing such early oncogenic events, thereby completely inhibiting the oncogenic actions of the constitutively active oncogenes and subsequent tumor foci formation in the host animals.

Our results suggested that the Y-located *RBMY* gene could possess dual oncogenic functions, ie being a tumor suppressor and proto-oncogene depending on its spatiotemporal and expression levels, in hepatocarcinogenesis (Figure S1). With high expression at the initiation stage, RBMY could suppress pro-oncogenic pathways, thereby serving as a male-specific tumor suppressor as its early effects. Surviving tumor cells could have evolved to adapt proliferative mode, thereby promoting HCC progression as its chronic effects. Preliminary data mining analyses of TCGA dataset revealed that, in clinical HCC samples, RBMY is co-expressed with various oncogenic genes whose expression levels are negatively correlated with survival ratio in patients with HCC, while those genes were not upregulated by RBMY overexpression in HuH-7 cells (Figure S2 and Table S2). These observations suggested that RBMY expression may lead to or be related with the activation of various oncogenic genes during processes of adaptation to the proliferative mode under clinical conditions. Future analyses of the RBMY expression in dysplastic nodules/premalignant lesions would provide information regarding the potential roles of RBMY at the early phase of hepatocarcinogenesis.

Recent studies on a variety of proto-oncogenes have suggested similar dual functions as tumor suppressors and oncogenes, and these have been termed double-agent genes, eg *NOTCHs*, *P21/CDKN1A*, *P27/CDKN1B*, *TGF-β*, and *WT1*.[87-89] Our results suggest that RBMY could be also one of these double-agent genes, suppressing and promoting hepatocarcinogenesis.

ACKNOWLEDGMENTS

The work was partially supported by a grant (CA150248) from the Peer-Reviewed Cancer Research Program of the Department of Defense, and a Merit Grant (1 IO1BX004446) from the Department of Veterans Affairs. Dr. Lau is the recipient of a Research Career Scientist award (1 IK6BX004854) from the Department of Veterans Affairs. We thank Dr. Luyi Li for technical assistance.

DISCLOSURE

The authors have no conflict of interest.

ORCID

Xin Chen https://orcid.org/0000-0002-9588-0164
Yun-Fai Chris Lau https://orcid.org/0000-0002-9119-7050

REFERENCES

1. Global Burden of Disease Cancer, Collaboration. Global, Regional, and National Cancer Incidence, Mortality, Years of Life Lost, Years Lived With Disability, and Disability-Adjusted Life-Years for 29 Cancer Groups, 1990 to 2016: a systematic analysis for the global burden of disease study. *JAMA Oncol*. 2018;4:1553-1568.
2. Bray F, Ferlay J, Soerjomataram I, Siegel RL, Torre LA, Jemal A. Global cancer statistics 2018: GLOBOCAN estimates of incidence and mortality worldwide for 36 cancers in 185 countries. *CA Cancer J Clin*. 2018;68:394-424.
3. World Cancer Research Fund International. *Liver cancer statistics*. 2019; https://www.wcrf.org/dietandcancer/cancer-trends/liver-cancer-statistics
4. Yang JD, Hainaut P, Gores GJ, Amadou A, Plymoth A, Roberts LR. A global view of hepatocellular carcinoma: trends, risk, prevention and management. *Nat Rev Gastroenterol Hepatol*. 2019;16:589-604.
5. El-Serag HB, Rudolph KL. Hepatocellular carcinoma: epidemiology and molecular carcinogenesis. *Gastroenterology*. 2007;132:2557-2576.
6. Liu P, Xie S-H, Hu S, et al. Age-specific sex difference in the incidence of hepatocellular carcinoma in the United States. *Oncotarget*. 2017;8:68131-68137.
7. Wong MCS, Jiang JY, Goggins WB, et al. International incidence and mortality trends of liver cancer: a global profile. *Sci Rep*. 2017;7:45846.
8. Cheung OK, Cheng AS. Gender differences in adipocyte metabolism and liver cancer progression. *Front Genet*. 2016;7:168.
9. Hartwell HJ, Petrosky KY, Fox JG, Horseman ND, Rogers AB. Prolactin prevents hepatocellular carcinoma by restricting innate immune activation of c-Myc in mice. *Proc Natl Acad Sci USA*. 2014;111:11455-11460.
10. Naugler WE, Sakurai T, Kim S, et al. Gender disparity in liver cancer due to sex differences in MyD88-dependent IL-6 production. *Science*. 2007;317:121-124.
11. Clocchiatti A, Cora E, Zhang Y, Dotto GP. Sexual dimorphism in cancer. *Nat Rev Cancer*. 2016;16:330-339.
12. Yeh SH, Chen PJ. Gender disparity of hepatocellular carcinoma: the roles of sex hormones. *Oncology*. 2010;78(Suppl 1):172-179.
13. Ma WL, Lai HC, Yeh S, Cai X, Chang C. Androgen receptor roles in hepatocellular carcinoma, fatty liver, cirrhosis and hepatitis. *Endocr Relat Cancer*. 2014;21:R165-R182.
14. Kido T, Lau YC. Identification of a TSPY co-expression network associated with DNA hypomethylation and tumor gene expression in somatic cancers. *J Genet Genomics*. 2016;43:577-585.
15. Kido T, Lau YF. Roles of the Y chromosome genes in human cancers. *Asian J Androl*. 2015;17:373-380.
16. Yin Y-H, Li Y-Y, Qiao H, et al. TSPY is a cancer testis antigen expressed in human hepatocellular carcinoma. *Br J Cancer*. 2005;93:458-463.
17. Udali S, Guarini P, Ruzzenente A, et al. DNA methylation and gene expression profiles show novel regulatory pathways in hepatocellular carcinoma. *Clin Epigenetics*. 2015;7:43.
18. Li S, Mo C, Huang S, et al. Over-expressed Testis-specific Protein Y-encoded 1 as a novel biomarker for male hepatocellular carcinoma. *PLoS One*. 2014;9:e89219.
19. Kido T, Lau YC. The Y-linked proto-oncogene TSPY contributes to poor prognosis of the male hepatocellular carcinoma patients by promoting the pro-oncogenic and suppressing the anti-oncogenic gene expression. *Cell Biosci*. 2019;9:22.
20. Chua HH, Tsuei DJ, Lee PH, et al. RBMY, a novel inhibitor of glycogen synthase kinase 3beta, increases tumor stemness and predicts poor prognosis of hepatocellular carcinoma. *Hepatology*. 2015;62:1480-1496.
21. Tsuei D-J, Lee P-H, Peng H-Y, et al. Male germ cell-specific RNA binding protein RBMY: a new oncogene explaining male predominance in liver cancer. *PLoS One*. 2011;6:e26948.

22. Affara NA, Lau YF, Briggs H, et al. Report and abstracts of the first international workshop on Y chromosome mapping 1994. Cambridge, England, April 2–5, 1994. *Cytogenet Cell Genet*. 1994;67:359-402.
23. Elliott DJ, Millar MR, Oghene K, et al. Expression of RBM in the nuclei of human germ cells is dependent on a critical region of the Y chromosome long arm. *Proc Natl Acad Sci USA*. 1997;94:3848-3853.
24. Elliott DJ, Bourgeois CF, Klink A, Stevenin J, Cooke HJ. A mammalian germ cell-specific RNA-binding protein interacts with ubiquitously expressed proteins involved in splice site selection. *Proc Natl Acad Sci USA*. 2000;97:5717-5722.
25. Liu Y, Bourgeois CF, Pang S, et al. The germ cell nuclear proteins hnRNP G-T and RBMY activate a testis-specific exon. *PLoS Genet*. 2009;5:e1000707.
26. Zeng M, Liang S, Zhao S, et al. Identifying mRNAs bound by human RBMY protein in the testis. *J Reprod Dev*. 2011;57:107-112.
27. Dreumont N, Bourgeois CF, Lejeune F, et al. Human RBMY regulates germline-specific splicing events by modulating the function of the serine/arginine-rich proteins 9G8 and Tra2-{beta}. *J Cell Sci*. 2010;123:40-50.
28. Cheung HH, Yang Y, Lee TL, Rennert O, Chan WY. Hypermethylation of genes in testicular embryonal carcinomas. *Br J Cancer*. 2016;114:230-236.
29. Sampath Kumar A, Seah MK, Ling KY, et al. Loss of maternal Trim28 causes male-predominant early embryonic lethality. *Genes Dev*. 2017;31:12-17.
30. Gossen M, Freundlieb S, Bender G, Muller G, Hillen W, Bujard H. Transcriptional activation by tetracyclines in mammalian cells. *Science*. 1995;268:1766-1769.
31. Kido T, Li Y, Tanaka Y, Dahiya R, Chris Lau YF. The X-linked tumor suppressor TSPX downregulates cancer-drivers/oncogenes in prostate cancer in a C-terminal acidic domain dependent manner. *Oncotarget*. 2019;10:1491-1506.
32. Huang DW, Sherman BT, Tan Q, et al. DAVID Bioinformatics Resources: expanded annotation database and novel algorithms to better extract biology from large gene lists. *Nucleic Acids Res*. 2007;35:W169-175.
33. Kanehisa M, Furumichi M, Tanabe M, Sato Y, Morishima K. KEGG: new perspectives on genomes, pathways, diseases and drugs. *Nucleic Acids Res*. 2017;45:D353-D361.
34. Ho C, Wang C, Mattu S, et al. AKT (v-akt murine thymoma viral oncogene homolog 1) and N-Ras (neuroblastoma ras viral oncogene homolog) coactivation in the mouse liver promotes rapid carcinogenesis by way of mTOR (mammalian target of rapamycin complex 1), FOXM1 (forkhead box M1)/SKP2, and c-Myc pathways. *Hepatology*. 2012;55:833-845.
35. Chen X, Calvisi DF. Hydrodynamic transfection for generation of novel mouse models for liver cancer research. *Am J Pathol*. 2014;184:912-923.
36. Hu J, Che LI, Li L, et al. Co-activation of AKT and c-Met triggers rapid hepatocellular carcinoma development via the mTORC1/FASN pathway in mice. *Sci Rep*. 2016;6:20484.
37. Buganim Y, Itskovich E, Hu Y-C, et al. Direct reprogramming of fibroblasts into embryonic Sertoli-like cells by defined factors. *Cell Stem Cell*. 2012;11:373-386.
38. Li Y, Zhang DJ, Qiu Y, Kido T, Lau YC. The Y-located proto-oncogene TSPY exacerbates and its X-homologue TSPX inhibits transactivation functions of androgen receptor and its constitutively active variants. *Hum Mol Genet*. 2017;26:901-912.
39. Kido T, Lau YF. The rat Tspy is preferentially expressed in elongated spermatids and interacts with the core histones. *Biochem Biophys Res Commun*. 2006;350:56-67.
40. Kido T, Lo R-L, Li Y, et al. The potential contributions of a Y-located protooncogene and its X homologue in sexual dimorphisms in hepatocellular carcinoma. *Hum Pathol*. 2014;45:1847-1858.
41. Kido T, Lau YF. The Y-located gonadoblastoma gene TSPY amplifies its own expression through a positive feedback loop in prostate cancer cells. *Biochem Biophys Res Commun*. 2014;446:206-211.
42. Liao Y, Smyth GK, Shi W. featureCounts: an efficient general purpose program for assigning sequence reads to genomic features. *Bioinformatics*. 2014;30:923-930.
43. Sun J, Nishiyama T, Shimizu K, Kadota K. TCC: an R package for comparing tag count data with robust normalization strategies. *BMC Bioinformatics*. 2013;14:219.
44. Fabregat A, Jupe S, Matthews L, et al. The reactome pathway knowledgebase. *Nucleic Acids Res*. 2018;46:D649-D655.
45. Jassal B, Matthews L, Viteri G, et al. The reactome pathway knowledgebase. *Nucleic Acids Res*. 2020;48:D498-D503.
46. Goldman M, Craft B, Kamath A, Brooks AN, Zhu J, Haussler D. The UCSC Xena Platform for cancer genomics data visualization and interpretation. *bioRxiv*. 2018. https://doi.org/10.1101/326470.
47. Uhlen M, Zhang C, Lee S, et al. A pathology atlas of the human cancer transcriptome. *Science*. 2017;357:eaan2507.
48. Chen C, Cao F, Bai L, et al. IKKbeta enforces a LIN28B/TCF7L2 positive feedback loop that promotes cancer cell stemness and metastasis. *Cancer Res*. 2015;75:1725-1735.
49. Pang M, Wu G, Hou X, et al. LIN28B promotes colon cancer migration and recurrence. *PLoS One*. 2014;9:e109169.
50. Takata H, Kudo M, Yamamoto T, et al. Increased expression of PDIA3 and its association with cancer cell proliferation and poor prognosis in hepatocellular carcinoma. *Oncol Lett*. 2016;12:4896-4904.
51. Shafizadeh N, Ferrell LD, Kakar S. Utility and limitations of glypican-3 expression for the diagnosis of hepatocellular carcinoma at both ends of the differentiation spectrum. *Mod Pathol*. 2008;21:1011-1018.
52. Hutter C, Zenklusen JC. The cancer genome atlas: creating lasting value beyond its data. *Cell*. 2018;173:283-285.
53. Pan D. The hippo signaling pathway in development and cancer. *Dev Cell*. 2010;19:491-505.
54. Carethers JM. Intersection of transforming growth factor-beta and Wnt signaling pathways in colorectal cancer and metastasis. *Gastroenterology*. 2009;137:33-36.
55. Brown MD, Sacks DB. Protein scaffolds in MAP kinase signalling. *Cell Signal*. 2009;21:462-469.
56. Manning BD, Cantley LC. AKT/PKB signaling: navigating downstream. *Cell*. 2007;129:1261-1274.
57. Hollander MC, Blumenthal GM, Dennis PA. PTEN loss in the continuum of common cancers, rare syndromes and mouse models. *Nat Rev Cancer*. 2011;11:289-301.
58. Calvisi DF, Ladu S, Gorden A, et al. Ubiquitous activation of Ras and Jak/Stat pathways in human HCC. *Gastroenterology*. 2006;130:1117-1128.
59. Whittaker S, Marais R, Zhu AX. The role of signaling pathways in the development and treatment of hepatocellular carcinoma. *Oncogene*. 2010;29:4989-5005.
60. Calvisi DF, Wang C, Ho C, et al. Increased lipogenesis, induced by AKT-mTORC1-RPS6 signaling, promotes development of human hepatocellular carcinoma. *Gastroenterology*. 2011;140:1071-1083.
61. Yang S, Liu G. Targeting the Ras/Raf/MEK/ERK pathway in hepatocellular carcinoma. *Oncol Lett*. 2017;13:1041-1047.
62. De Luca A, Maiello MR, D'Alessio A, Pergameno M, Normanno N. The RAS/RAF/MEK/ERK and the PI3K/AKT signalling pathways: role in cancer pathogenesis and implications for therapeutic approaches. *Expert Opin Ther Targets*. 2012;16(Suppl 2):S17-27.
63. Song M, Bode AM, Dong Z, Lee MH. AKT as a therapeutic target for cancer. *Cancer Res*. 2019;79:1019-1031.
64. Pylayeva-Gupta Y, Grabocka E, Bar-Sagi D. RAS oncogenes: weaving a tumorigenic web. *Nat Rev Cancer*. 2011;11:761-774.
65. Wang C, Cigliano A, Delogu S, et al. Functional crosstalk between AKT/mTOR and Ras/MAPK pathways in hepatocarcinogenesis: implications for the treatment of human liver cancer. *Cell Cycle*. 2013;12:1999-2010.
66. Lahn BT, Pearson NM, Jegalian K. The human Y chromosome, in the light of evolution. *Nat Rev Genet*. 2001;2:207-216.

67. Bellott DW, Hughes JF, Skaletsky H, et al. Mammalian Y chromosomes retain widely expressed dosage-sensitive regulators. *Nature*. 2014;508:494-499.
68. Skaletsky H, Kuroda-Kawaguchi T, Minx PJ, et al. The male-specific region of the human Y chromosome is a mosaic of discrete sequence classes. *Nature*. 2003;423:825-837.
69. Hughes JF, Skaletsky H, Pyntikova T, et al. Chimpanzee and human Y chromosomes are remarkably divergent in structure and gene content. *Nature*. 2010;463:536-539.
70. Kashimada K, Koopman P. Sry: the master switch in mammalian sex determination. *Development*. 2010;137:3921-3930.
71. Lau YC, Li Y, Kido T. Battle of the sexes: contrasting roles of testis-specific protein Y-encoded (TSPY) and TSPX in human oncogenesis. *Asian J Androl*. 2019;21:260-269.
72. Li Y, Lau YF. TSPY and its X-encoded homologue interact with cyclin B but exert contrasting functions on cyclin-dependent kinase 1 activities. *Oncogene*. 2008;27:6141-6150.
73. Lau YF, Li Y, Kido T. Role of the Y-located putative gonadoblastoma gene in human spermatogenesis. *Syst Biol Reprod Med*. 2011;57:27-34.
74. Li Y, Kido T, Garcia-Barcelo MM, Tam PK, Tabatabai ZL, Lau YF. SRY interference of normal regulation of the RET gene suggests a potential role of the Y-chromosome gene in sexual dimorphism in Hirschsprung disease. *Hum Mol Genet*. 2015;24:685-697.
75. Kido T, Sun Z, Lau YC. Aberrant activation of the human sex-determining gene in early embryonic development results in postnatal growth retardation and lethality in mice. *Sci Rep*. 2017;7:4113.
76. Wang SH, Chen PJ, Yeh SH. Gender disparity in chronic hepatitis B: mechanisms of sex hormones. *J Gastroenterol Hepatol*. 2015;30:1237-1245.
77. Ma WL, Jeng LB, Lai HC, Liao PY, Chang C. Androgen receptor enhances cell adhesion and decreases cell migration via modulating beta1-integrin-AKT signaling in hepatocellular carcinoma cells. *Cancer Lett*. 2014;351:64-71.
78. Kalra M, Mayes J, Assefa S, Kaul AK, Kaul R. Role of sex steroid receptors in pathobiology of hepatocellular carcinoma. *World J Gastroenterol*. 2008;14:5945-5961.
79. Li Z, Tuteja G, Schug J, Kaestner KH. Foxa1 and Foxa2 are essential for sexual dimorphism in liver cancer. *Cell*. 2012;148:72-83.
80. Lau YF. Gonadoblastoma, testicular and prostate cancers, and the TSPY gene. *Am J Hum Genet*. 1999;64:921-927.
81. Tsuei D-J, Hsu H-C, Lee P-H, et al. RBMY, a male germ cell-specific RNA-binding protein, activated in human liver cancers and transforms rodent fibroblasts. *Oncogene*. 2004;23:5815-5822.
82. Delbridge ML, Lingenfelter PA, Disteche CM, Graves JA. The candidate spermatogenesis gene RBMY has a homologue on the human X chromosome. *Nat Genet*. 1999;22:223-224.
83. Adamson B, Smogorzewska A, Sigoillot FD, King RW, Elledge SJ. A genome-wide homologous recombination screen identifies the RNA-binding protein RBMX as a component of the DNA-damage response. *Nat Cell Biol*. 2012;14:318-328.
84. Matsunaga S, Takata H, Morimoto A, et al. RBMX: a regulator for maintenance and centromeric protection of sister chromatid cohesion. *Cell Rep*. 2012;1:299-308.
85. Heinrich B, Zhang Z, Raitskin O, et al. Heterogeneous nuclear ribonucleoprotein G regulates splice site selection by binding to CC(A/C)-rich regions in pre-mRNA. *J Biol Chem*. 2009;284:14303-14315.
86. Shashi V, Xie P, Schoch K, et al. The RBMX gene as a candidate for the Shashi X-linked intellectual disability syndrome. *Clin Genet*. 2015;88:386-390.
87. Shen L, Shi Q, Wang W. Double agents: genes with both oncogenic and tumor-suppressor functions. *Oncogenesis*. 2018;7:25.
88. Bashyam MD, Animireddy S, Bala P, Naz A, George SA. The Yin and Yang of cancer genes. *Gene*. 2019;704:121-133.
89. Emon B, Bauer J, Jain Y, Jung B, Saif T. Biophysics of tumor microenvironment and cancer metastasis – A mini review. *Comput Struct Biotechnol J*. 2018;16:279-287.

SUPPORTING INFORMATION

Additional supporting information may be found online in the Supporting Information section.

How to cite this article: Kido T, Tabatabai ZL, Chen X, Lau Y-FC. Potential dual functional roles of the Y-linked RBMY in hepatocarcinogenesis. *Cancer Sci*. 2020;111:2987–2999. https://doi.org/10.1111/cas.14506